

Zebrafish brain regeneration - Independent Project

Vishnu Mothukuri, 2021502

B.Tech
IIITD'25

Gene trend sheet and DAVID analysis

K30

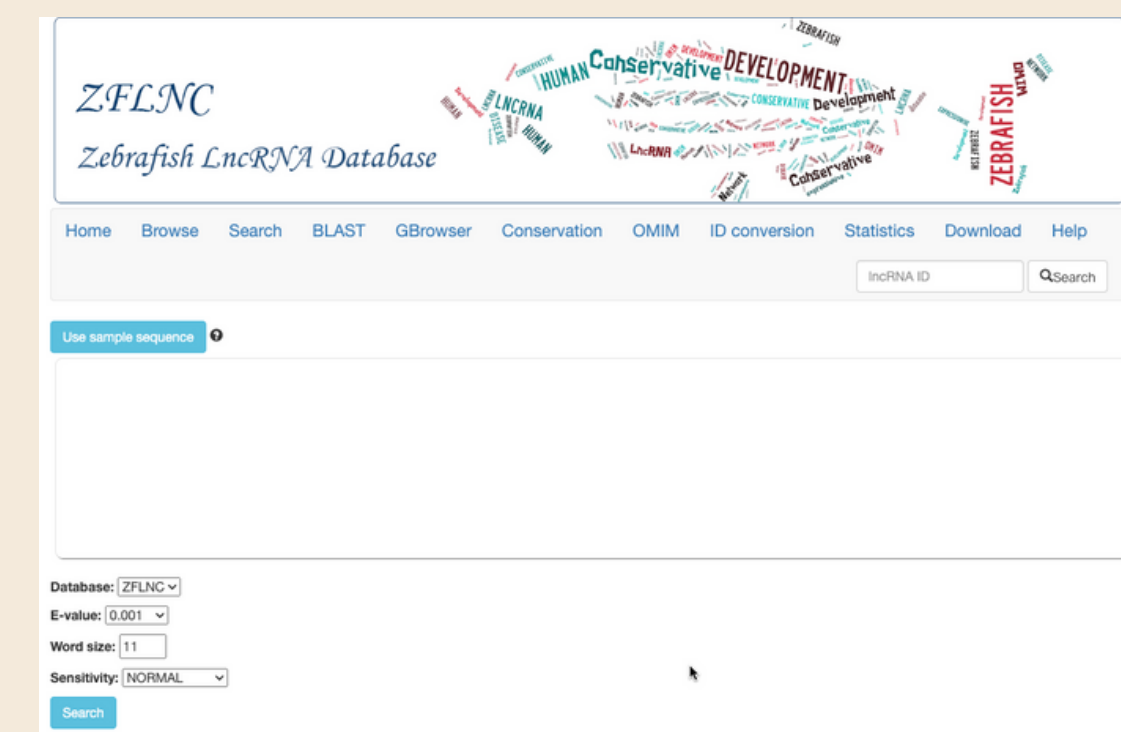
	A	B	C	D	E	F	G	H	
1	gene_name	le	t	sco	ta	re	log2FoldChange (Day 1)	log2FoldChange (Day 4)	log2FoldChange (Day 7)
2	ciarta					2.972747967	5.225410529	4.233870875	
3	per1a					2.889495482	5.034335211	4.163051689	
4	LOC100331278					2.5847845	3.273630316	0.28812482	
5	nr1d1					2.489183629	4.085183577	2.801412891	
6	cipca					2.422034847	4.334022029	3.607614358	
7	nr1d2b					2.415998304	2.622653045	2.078527679	
8	agtr1b					2.392097383	2.415683003	1.771315382	
9	LOC559843					2.342233882	2.602669751	2.214095914	
10	per1b					2.31021185	3.817956529	3.19944221	
11	LOC110439135					2.222092032	3.059477058	1.221800401	
12	LOC100329651					2.211823483	2.43259291	2.279335994	
13	Ictlb					2.169483204	2.286001866	1.953267874	
14	LOC110439303					2.086924647	2.210134944	2.043770976	
15	si:dkey-195m11.11					2.035323944	2.511571091	1.06954296	
16	gbp1					1.983430269	2.080367698	1.446996237	
17	bhlhe41					1.920341336	3.533076127	3.26829971	
18	LOC100149352					1.897804909	2.241746235	1.825669648	
19	si:ch211-132b12.7					1.88067006	3.773958403	2.499168902	
20	zgc:173544					1.867714567	2.460037726	1.677164012	
21	bard1					1.819262672	2.122623646	1.30396326	
22	and2					1.807129624	3.278569433	3.168779217	
23	zgc:123299					1.783018002	2.419817517	1.491650609	
24	rlbp1a					1.777472588	2.32253659	1.361790334	
25	hsf2					1.772136405	2.078344147	1.282013953	
26	LOC110438689					1.758161916	2.172003902	1.497072283	
27	setd8b					1.754649814	2.70103615	2.128473271	
28	LOC567978					1.700169597	3.000581069	2.086297229	
29	aurka					1.649481701	3.203294346	2.855100312	
30	LOC101885269					1.627849449	2.670429849	2.21220017	
31	igf3					1.584794304	2.893701907	2.401230029	
32	hmmr					1.584571473	1.82001973	1.435527587	
33	LOC110438894					1.573343158	1.931856889	1.314656294	
34	LOC101885916					1.566768238	1.620723639	1.473085318	
35	il4r.2					1.564563597	1.746567372	1.259778476	
36	LOC101887150					1.553296848	1.569968825	0.7172004341	

Global Enrichment Analysis Results												
Category			Term			Count			PValue			
Category	Term	Count	%	PValue	Genes	List Total	Pop Hits	Pop Total	Fold Enrichment	Bonferroni	Benjamini	FDR
GOTERM_BP_D	GO:0007049-ce	18	4.591836734693	3.50E-09	CDT1, UHFR1, SPICE1, C	189	269	17990	6.369268897149	1.72E-06	1.72E-06	1.71E-06
UP_KW_BIOL	KW-0131-Cell c	18	4.591836734693	4.09E-09	CDT1, UHFR1, SPICE1, C	57	280	5022	5.663909774436	1.43E-07	1.43E-07	1.43E-07
UP_KW_MOLEC	KW-0238-DNA-I	25	6.377551020408	4.32E-05	TOP2A, CREB5B, UHFR1, S	110	874	9466	2.461514458081	0.002159196412	0.002161484116	0.002161484116
GOTERM_BP_D	GO:0000278-mi	8	2.040816326530	5.04E-05	ASPM, CDT1, CHAF1B, C	189	92	17990	8.276972624798	0.024505137275	0.012379666671	0.012278813
INTERPRO	IPR018525:Minic	4	1.020408163265	9.52E-05	MCM4, MCM5, MCM6, M	185	9	17276	41.50390390390	0.036556629557	0.026391410156	0.026391410156
GOTERM_BP_D	GO:0032922-cir	6	1.530612244897	1.03E-04	PER3, BHLHE41, PER1B, P	189	45	17990	12.69135802469	0.049348816555	0.016834204522	0.016697062
INTERPRO	IPR001208:Minic	4	1.020408163265	1.35E-04	MCM4, MCM5, MCM6, M	185	10	17276	37.3535135135	0.051417376094	0.026391410156	0.026391410156
GOTERM_CC_D	GO:0042555-M	4	1.020408163265	1.51E-04	MCM4, MCM5, MCM6, M	203	10	18265	35.99014778325	0.018554760861	0.018727645499	0.018727645499
SMART	SM00350:MCM	4	1.020408163265	1.68E-04	MCM4, MCM5, MCM6, M	110	10	9474	34.45090909090	0.016625121515	0.016763464677	0.016763464677
KEGG_PATHWA	dre04110:Cell cy	10	2.551020408163	1.94E-04	CDT1, CDC14AA, E2F1, I	79	190	7204	4.799467021982	0.014801604278	0.014910797215	0.014910797215
UP_SEQ_FEAT	DOMAIN:MCM	4	1.020408163265	2.09E-04	MCM4, MCM5, MCM6, M	302	10	24416	32.33907284766	0.055996493945	0.057619383485	0.057619383485
GOTERM_MF_D	GO:0003677-Dt	33	8.418367346936	2.15E-04	TOP2A, CREB5B, FOXE3, C	183	1529	16808	1.982309234579	0.051039550837	0.052382533955	0.051738486
GOTERM_BP_D	GO:0000727-dc	4	1.020408163265	2.97E-04	MCM4, MCM5, MCM6, M	189	13	17990	29.28774928774	0.136126007705	0.036502308475	0.036204937
INTERPRO	IPR022728:Peric	3	0.765306122448	6.67E-04	PER3, PER1B, PER1A	185	4	17276	70.03783783783	0.229774725513	0.086995034186	0.086995034186
GOTERM_MF_D	GO:0001222-tra	3	0.765306122448	6.90E-04	PER3, PER1B, PER1A	183	4	16808	68.88524590163	0.154941961948	0.072006610110	0.071121282
GOTERM_MF_D	GO:0000978-RN	24	6.122448979597	0.001171823585	CREB5B, FOXE3, STAT3, C	183	1063	16808	2.073685671545	0.248806957316	0.072006610110	0.071121282
GOTERM_MF_D	GO:0003678-Dt	5	1.27551020408	0.001180436231	XRCC5, MCM4, MCM5, M	183	43	16808	10.67988308552	0.250385775985	0.072006610110	0.071121282
GOTERM_BP_D	GO:0006270-Dt	4	1.020408163265	0.001300333747	MCM4, MCM5, MCM6, M	189	21	17990	18.13051146384	0.472802753258	0.127692774005	0.126652507
GOTERM_BP_D	GO:0000122-ne	10	2.551020408163	0.001734644190	PER3, NR1D2B, UHFR1, C	189	261	17990	3.646941961118	0.574370491885	0.141951716236	0.140795286
UP_KW_MOLEC	KW-0347-Helice	7	1.785714285714	0.002161781636	LOC101886064, XRCC5, C	110	116	9466	5.192946708463	0.102557370281	0.054044540911	0.054044540911
GOTERM_MF_D	GO:0003700-tra	16	4.08163265306	0.002238876782	CREB5B, FOXE3, STAT3, C	183	599	16808	2.453342091095	0.421257934135	0.109257187003	0.107913860
GOTERM_BP_D	GO:0032508-Dt	4	1.020408163265	0.002446382151	MCM4, MCM5, MCM6, M	189	26	17990	14.64387464387	0.700336374314	0.171596233734	0.170198301
GOTERM_BP_D	GO:0006268-Dt	3	0.765306122448	0.004626050756	MCM4, MCM6, MCM2	189	10	17990	28.555555555555	0.897848446474	0.283923865173	0.281610839
GOTERM_BP_D	GO:0006954-inf	7	1.785714285714	0.006570926663	UHFR1, IL1B, C5AR1, AD	189	159	17990	4.19054274400	0.960975445914	0.305200802992	0.302714442
GOTERM_BP_D	GO:0045892-ne	7	1.785714285714	0.006570926663	BHLHE41, SI:CH211-132I	189	159	17990	4.19054274400	0.960975445914	0.305200802992	0.302714442
GOTERM_BP_D	GO:0019221-cy	5	1.27551020408	0.00683749253	CRLF1A, IL10RA, IL1B, S	189	72	17990	6.610082304526	0.965802400961	0.305200802992	0.302714442
GOTERM_MF_D	GO:0017116-sir	3	0.765306122448	0.007166169938	MCM4, MCM5, MCM2	183	12	16808	22.96174863387	0.827065219224	0.291424244155	0.287841159
KEGG_PATHWA	dre03030:DNA re	4	1.020408163265	0.007846248918	MCM4, MCM5, MCM6, M	79	38	7204	9.598934043970	0.454767973234	0.302080583373	0.302080583
INTERPRO	IPR004827:Basi	5	1.27551020408	0.009213428115	DBPA, CREB5B, NRL, NF	185	77	17276	6.063882063882	0.973194508232	0.845687642402	0.845687642402
SMART	SM00338:BRLZ	5	1.27551020408	0.010294865933	DBPA, CREB5B, NRL, NF	110	74	9474	5.819410319410	0.644710546499	0.416335176672	0.416335176672
GOTERM_BP_D	GO:0073265-h	2	1.785714285714	0.01042312170621	STAT3, F527, F528	189	15	17000	1.02320232023202	0.204250234466	0.302080583373	0.302080583373

ZFLNC BLAST

gene name	gene type	100% identity	KEGG annotation	
apip	protein coding	-		
birc6-as2	ncRNA	-		
cald1a	protein coding	ZFLNCT01905 (96.2%)	Yes	
crhr2	protein coding	ZFLNCT19948	No	
crsp7	protein coding	ZFLNCT01414	No	
ctbs	polymorphic_pseudogene	-		
cyp19a1b	protein coding	ZFLNCT02442 (94%)	Yes	
cyp2aa6	protein coding	ZFLNCT06181 (96.8%)	Yes	
dio3b	protein coding	ZFLNCT17563	Yes	ZFLNCT17564
dsg2.1	protein coding	ZFLNCT16829	Yes	
efcab6	protein coding	ZFLNCT20894	Yes	
fem1a	protein coding	ZFLNCT02075	Yes	
ipp	protein coding	ZFLNCT06000	No	
kcnip3a	processed_transcript	-		
mdh1ab	polymorphic_pseudogene	-		
mhc1zda	lincRNA	ZFLNCT00765	Yes	
mir140	miRNA	-		
mocos	protein coding	ZFLNCT11556	No	ZFLNCT11553
nadsyn1	protein coding	ZFLNCT13101 (97%)	Yes	
ndst2a	polymorphic_pseudogene	-		
oip5-as1	lincRNA	ZFLNCT11807	Yes	ZFLNCT11806
oxr1a	protein coding	-		
pcdh1g11	polymorphic_pseudogene	-		
pla1a	polymorphic_pseudogene	-		
pln	protein coding	ZFLNCT17312	Yes	ZFLNCT17313
rps20	protein coding	ZFLNCT07356	Yes	
rwdd3	protein coding	ZFLNCT01318	Yes	
rxrga	processed_transcript	-		
si:ch1073-325m22.2	processed_transcript	-		
si:ch211-214p16.1	ncRNA	ZFLNCT14798	Yes	ZFLNCT14797
si:ch211-2012.2	antisense	-		

- Downloaded Zebrafish gene data from Ensembl
- Obtained common lnc rna from NCBI search, gtf file, and degs list
- Ran BLASTN in ZFLNC to obtain identical ZF transcripts along with their KEGG annotation
- Took default word size of 11
- E-value as - 0.001

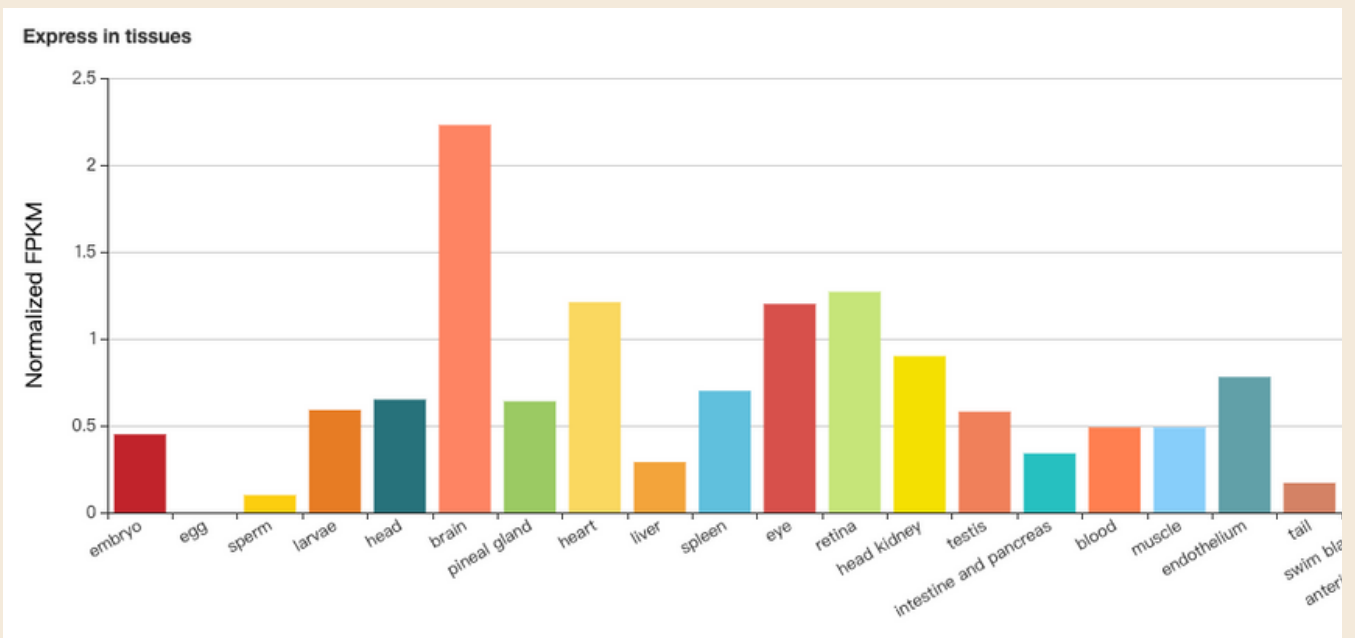


Brain related ncRNA transcripts

ZFLNCG04672

Basic Information

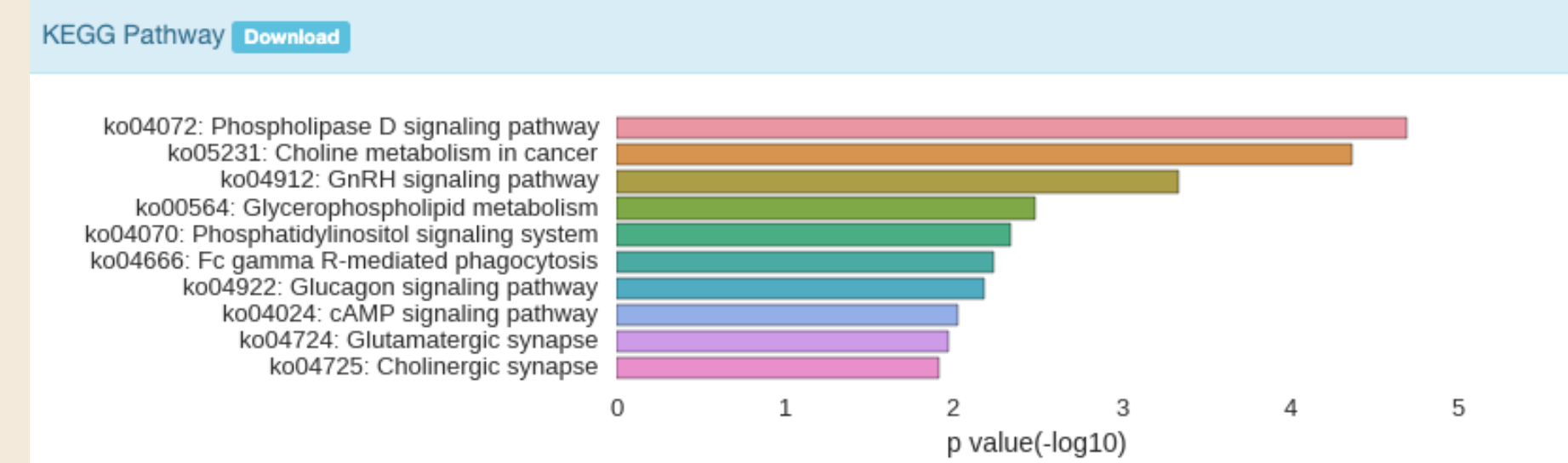
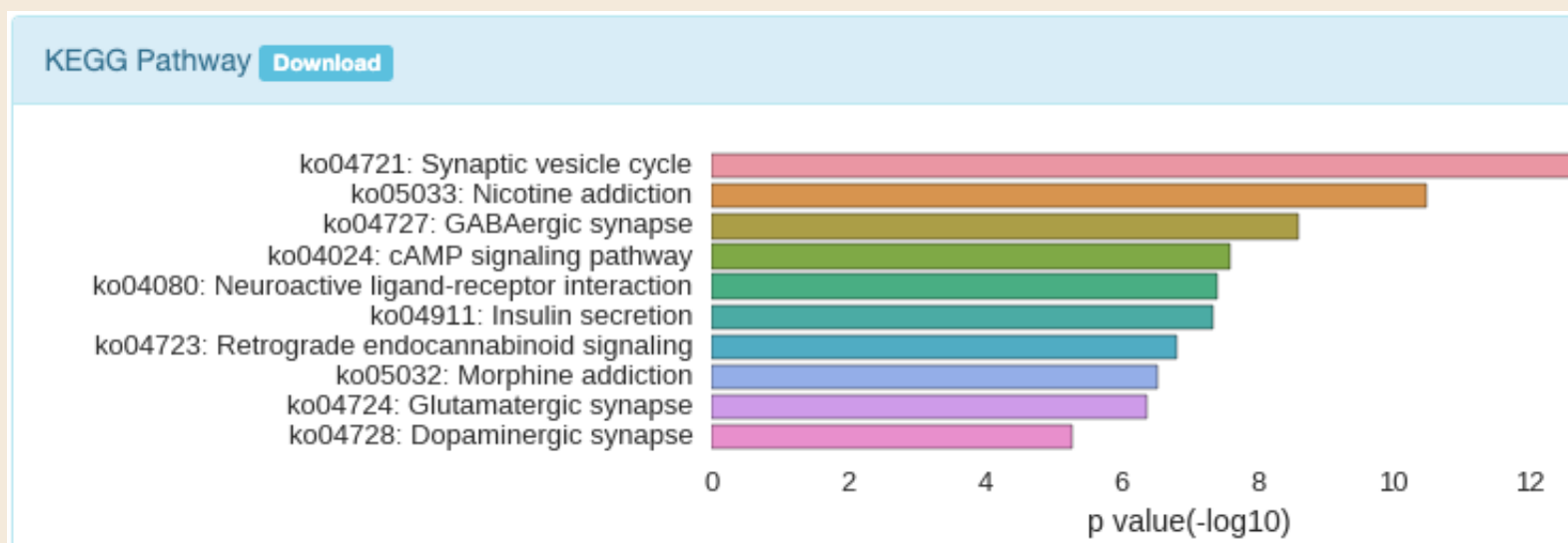
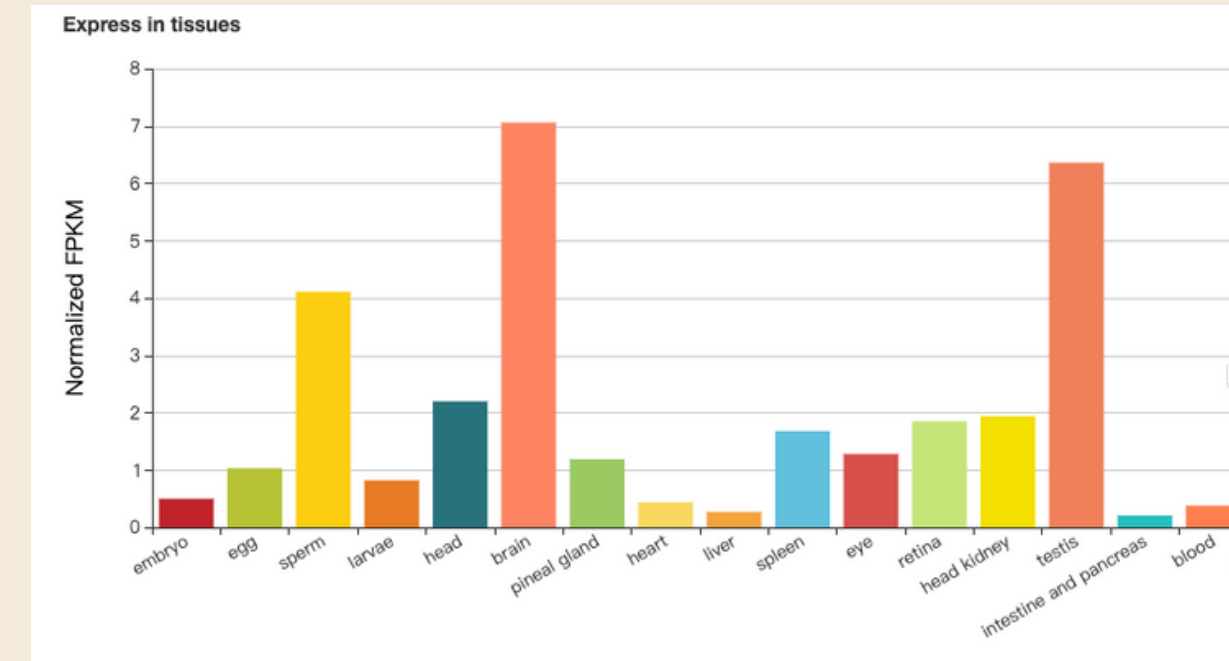
Chromosome: chr7
Start: 45659411
End: 45669869
Transcript: ZFLNCT07220 ZFLNCT07221 ZFLNCT07222
Known as: LOC103911411



ZFLNCG04657

Basic Information

Chromosome: chr7
Start: 43692355
End: 43833964
Transcript: ZFLNCT07196 ZFLNCT07197 ZFLNCT07198 ZFLNCT07199 ZFLNCT07200
Known as: LOC101886520



Annotation of uncharacterized genes (LOCs)

similarly performed gene annotation of brain related LOCs using ZFLNC database, for each trend

	A	B	C	D	E	F	G	H	I
1	gene name	gene type	transcript (100% identity)	annotation	brain related	H-G	log2FoldChange (Day 1)	log2FoldChange (Day 4)	log2FoldChange (Day 7)
2	LOC100535070	protein coding	ZFLNCT00826 (95.2%)	Yes	yes	3.701141025	-4.894914905	-1.19377388	-1.251575925
3	LOC110438058	protein coding	ZFLNCT00462	no		3.473454694	-3.104884034	0.3685706602	0.06421653204
4	LOC101883131	protein coding	-			2.928812175	-0.6376287107	2.291183464	0.9197080266
5	LOC103909700	protein coding	-			2.697444885	-1.675248625	1.02219626	-0.5645842576
6	LOC101882092	protein coding	-			2.223354044	0.169564799	2.392918843	1.856915319
7	LOC100007517	ncRNA	ZFLNCT02104	Yes	no	2.186593155	0.2344986669	2.421091822	0.7200359275
8	LOC108181236	protein coding	ZFLNCT18857	Yes	no	2.159904641	0.321758372	2.48166301	2.271655347
9	LOC100538151	protein coding	-			1.981800668	-1.27601841	0.705782258	-1.354525258
10	LOC108190667	ncRNA	-			1.937727281	-0.1427908385	1.794936443	1.065150534
11	LOC103912040	protein coding	ZFLNCT18927	Yes	no	1.930553695	-0.9655760252	0.9649776701	0.2558412465
12	LOC108179987	protein coding	ZFLNCT15443	no	no	1.907761482	-1.129584846	0.778176636	-0.0008210812654
13	LOC103911776	protein coding	-			1.87794586	-0.4316335602	1.446312299	1.217827363
14	LOC108191363	ncRNA	-			1.875365205	-1.180876019	0.6944891863	0.4355430473
15	LOC103911747	ncRNA	ZFLNCT09758	no	no	1.84871069	-1.047368965	0.8013417253	0.2145901759
16	LOC101883513	protein coding	-			1.845992668	-0.8409809858	1.005011683	0.6836659688
17	LOC110438063	ncRNA	ZFLNCT15050	no	no	1.838807513	1.234182868	3.072990381	1.555524672
18	LOC101884563	protein coding	ZFLNCT04358	Yes	no	1.826923867	-1.540889277	0.2860345901	0.2848779678
19	LOC103910812	protein coding	ZFLNCT04442	Yes	no	1.808332655	0.8069437555	2.615276411	2.028971978
20	LOC100002503	protein coding	-			1.795354209	-1.40967101	0.3856831999	0.144792073
21	LOC101885930	protein coding	ZFLNCT04403	Yes	no	1.766418227	-0.9007298033	0.8656884241	0.3815355495
22	LOC103909544	ncRNA	ZFLNCT15926 (99.2%)	Yes	yes	1.726558036	-1.344115233	0.3824428031	0.1641460897
23	LOC110439604	protein coding	ZFLNCT04441	no	no	1.702615487	0.757412523	2.46002801	1.635584633
24	LOC108183921	protein coding	-			1.685291811	-1.652264533	0.03302727745	-0.1026617889
25	LOC100150236	protein coding	-			1.562745971	-1.192993965	0.3697520054	-0.7278926175
26	LOC110437884	protein coding	-			1.531319845	-0.7372257521	0.7940940932	-0.04969957129
27	LOC10440206	ncRNA	-			1.518371854	-0.3984378886	1.119933965	0.7554013253
28	LOC110438218	protein coding	-			1.509257405	-0.05512201009	1.454135395	0.4948890315
29	LOC101885243	protein coding	-			1.491224784	-0.6954904742	0.7957343101	-0.3339024769
30	LOC101886581	ncRNA	ZFLNCT20008	Yes	yes	1.468990792	-1.658143719	-0.1891529265	-2.197504898
31	LOC100536577	protein coding	ZFLNCT04887	Yes	no	1.467136341	0.7558493168	2.222985658	1.461332985
32	LOC567909	protein coding	-			1.466524481	-0.193005481	1.273519	-0.5868495641
33	LOC101884650	protein coding	ZFLNCT04886	no	no	1.436963817	0.7652843851	2.202248202	1.320634431

ZF brain cancer data

	A	B	C	D	E	F	G	H	I	J
1	gene_name	seMe	log2FC_cancer	IfcSE	stat	pvalue	padj	log2FC_day1	log2FC_day4	log2FC_day7
2	CYTB	1933	0.03917843365	0.271396	0.144358	0.885217	0.95873	-0.2567611338	-0.7826541838	-0.8636220524
3	ND6	2429	0.04907091314	0.285648	0.171787	0.863604	0.95029	0.01541426754	-0.4310631517	-0.6295525513
4	ND5	7027	0.1970037548	0.266045	0.740487	0.459004	0.72835	-0.08033121999	-0.492348918	-0.6464573306
5	ND4	1009	0.0500550212	0.256183	0.19387	0.845089	0.94350	-0.17967151	-0.5433915352	-0.7872893076
6	ND4L	1103	0.2434801188	0.312098	0.780138	0.435309	0.70984	-0.3813374034	-0.8428889152	-1.175756942
7	ND3	2153	-0.336929035	0.382170	-0.881620	0.377982	0.65994	-0.7056532961	-0.9503948794	-1.030851164
8	COX3	3221	-0.3283022691	0.346004	-0.948838	0.342702	0.62856	-0.230782289	-0.400716198	-0.5530554039
9	ATP6	1724	-0.2278417525	0.318165	-0.7161110	0.473922	0.73858	-0.1552842299	-0.6309363777	-0.9695001368
10	ATP8	2033	0.108563099	0.282096	0.384844	0.700352	0.87925	-0.3874865622	-0.6242128304	-1.197062435
11	COX2	2742	-0.3079586417	0.371353	-0.829285	0.406942	0.68451	-0.109475159	-0.3394614314	-0.6596811543
12	COX1	7238	-0.1266141772	0.276456	-0.457989	0.646960	0.84946	-0.1873619604	-0.4385941325	-0.706228171
13	ND2	7371	-0.1018532145	0.281983	-0.361203	0.717947	0.88764	-0.3868055795	-0.6659752297	-0.8678580923
14	ND1	8325	-0.1341195405	0.259754	-0.5163310	0.605622	0.82411	-0.1176447834	-0.2973408402	-0.6189863539
15	gria1a	348.	0.3858857798	0.391395	0.985923	0.324170	0.61018	-0.07401702946	0.2499880234	0.1247393935
16	dlg1	5852	-0.7016686987	0.245841	-2.854148	0.004315	0.04043	0.2152632406	0.1032330812	0.1518656727
17	phb2b	186.	1.21821786	0.574287	2.121266	0.033899	0.16566		-2.895409373	
18	pde6d	239.	-0.4920697637	0.320861	-1.5335910	0.125130	0.36342		-2.262393928	
19	pex5la	59.2	-0.5728449078	0.542228	-1.056463	0.290756	0.57831	-0.4092054036	-0.630772934	-0.5903152123
20	cdh4	4261	-0.5156802443	0.178315	-2.891959	0.003828	0.03712	-0.04272043486	0.0916080583	0.1071144602
21	rbb4l	1007	-0.5502765664	0.328534	-1.674942	0.093945	0.30935	0.1590659491	-0.02989269436	0.1242800391
22	dgkh	9794	-0.1823741446	0.277068	-0.658226	0.510392	0.76406	0.259878887	0.6477668438	0.3402711991
23	vwa8	156.	0.001877709092	0.288160	0.006516	0.994800	0.99998	0.04182668101	-0.270061262	-0.150535732
24	slain1a	51.3	0.5842774069	0.379286	1.540466	0.123446	0.36152	-0.6392818125	0.03064616605	-0.3613940088
25	mycbp2	2997	0.07838097056	0.316593	0.247575	0.804462	0.92751	0.07439675801	0.3157878386	0.2805124519
26	itpr1a	82.6	0.8114536972	0.554171	1.464263	0.143121	0.39237	0.01991527523	0.11761083	-0.06311636041
27	sumf1	174.	-0.01683749959	0.340493	-0.049450	0.960560	0.98537	-0.7294875489	-0.5504106781	-0.2777952541
28	tsfm	104.	-0.3733042435	0.318977	-1.1703150	0.241873	0.52754	0.2221052048	0.6172830095	0.179672968
29	myl6	1502	-0.2308029816	0.286665	-0.805130	0.420744	0.69629	-0.2371617927	-0.4902218937	-0.2935099702
30	smarcc2	1368	-0.1714403661	0.200065	-0.8569210	0.391488	0.67233	-0.04516791745	-0.206993387	-0.1688609665
31	c1ql4b	153.	-0.4173213463	0.433730	-0.9621660	0.335965	0.62285	-0.3612546618	-0.6405129346	-0.1763820023
32	itgb7	106.	2.033092552	0.548631	3.705752	0.000210	0.00409	-0.4437393755	-0.9168816598	
33	espl1	119.	-0.7122148103	0.328597	-2.167440	0.030201	0.15430	-1.36022733	-1.018278437	0.03625164992
34	pfdn5	965.	-1.119930005	0.387619	-2.889250	0.003861	0.03733	-1.480632336	-1.41022399	-0.8550337304
35	lrp8	1736	0.1491447989	0.476218	0.313185	0.754139	0.90532	0.09935670741	0.6142861087	0.2010657553
36	mast2	3020	0.05002241763	0.255619	0.195691	0.844851	0.94330	0.1415311283	0.1876192498	-0.007149687326

+ ≡ exclusive_cancer ▼ exclusive_regeneration ▼ common ▼

Early Brain Regeneration resembles Brain Cancer

- Due to cellular similarities between tumor stroma and granulation tissue, cancers have long been described as wounds that do not heal
- Brain tumors are the most difficult to treat cancers and gliomas are the most frequently occurring types of tumors in the CNS
- Gliomas are classified from grade I to grade IV:
 - grade I being less aggressive
 - grade II-IV being malignant
 - GBM is classified as a grade IV glioma
- Mammalian neurogenesis is limited to only 2 regions of the forebrain, while ZF have 16 proliferative zones in their brain parenchyma
- Looked at the transcription profiles of 1dpl, 3dpl, and 14dpl of ZF telencephalon
- Compared them with low-grade glioma (LGG) and glioblastoma(GBM)

Brain Regeneration Resembles Brain Cancer at Its Early Wound Healing Stage and Diverges From Cancer Later at Its Proliferation and Differentiation Stages

 Yeliz Demirci^{1,2,3}  Guillaume Heger⁴  Esra Katkat^{1,2}  Irene Papathodorou⁵  Alvis Brazma⁵  Gunes Ozhan^{1,2*}

¹ Izmir Biomedicine and Genome Center (IBG), Dokuz Eylul University Health Campus, Inciralti-Balcova, Izmir, Turkey

² Izmir International Biomedicine and Genome Institute (IBG-Izmir), Dokuz Eylul University, Inciralti-Balcova, Izmir, Turkey

³ Wellcome Sanger Institute, Hinxton, United Kingdom

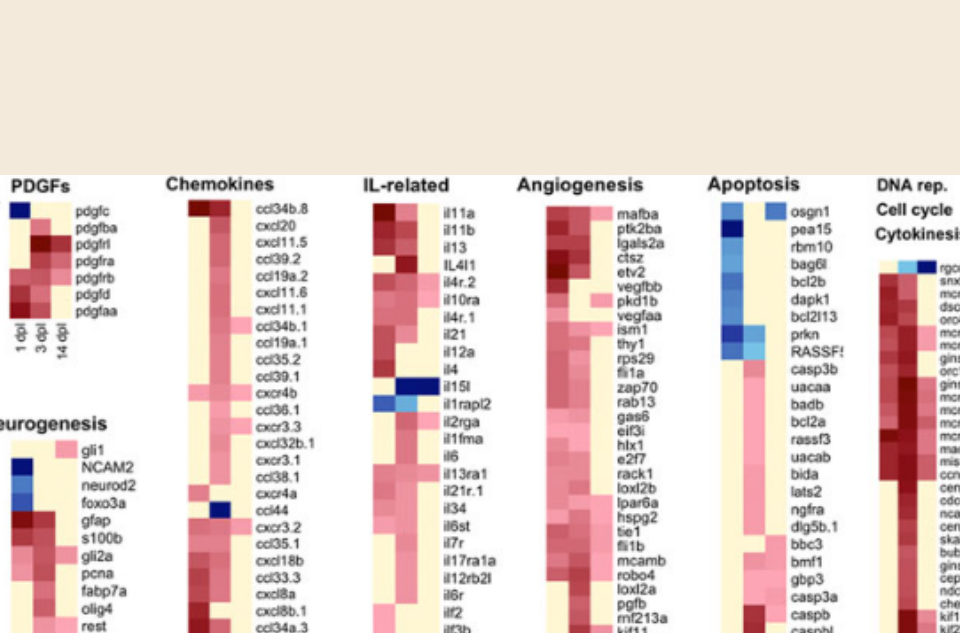
⁴ École Centrale de Nantes, Nantes, France

⁵ European Molecular Biology Laboratory-European Bioinformatics Institute (EMBL-EBI), Cambridge, United Kingdom

Gliomas are the most frequent type of brain cancers and characterized by continuous proliferation, inflammation, angiogenesis, invasion and dedifferentiation, which are also among the initiator and sustaining factors of brain regeneration during restoration of tissue integrity and function. Thus, brain regeneration and brain cancer should share more molecular mechanisms at early stages of regeneration where cell proliferation dominates. However, the mechanisms could diverge later when the regenerative response terminates, while cancer cells sustain proliferation. To test this hypothesis, we exploited the adult zebrafish that, in contrast to the mammals, can efficiently regenerate the brain in response to injury. By comparing transcriptome profiles of the regenerating zebrafish telencephalon at its three different stages, i.e., 1 day post-lesion (dpl)-early

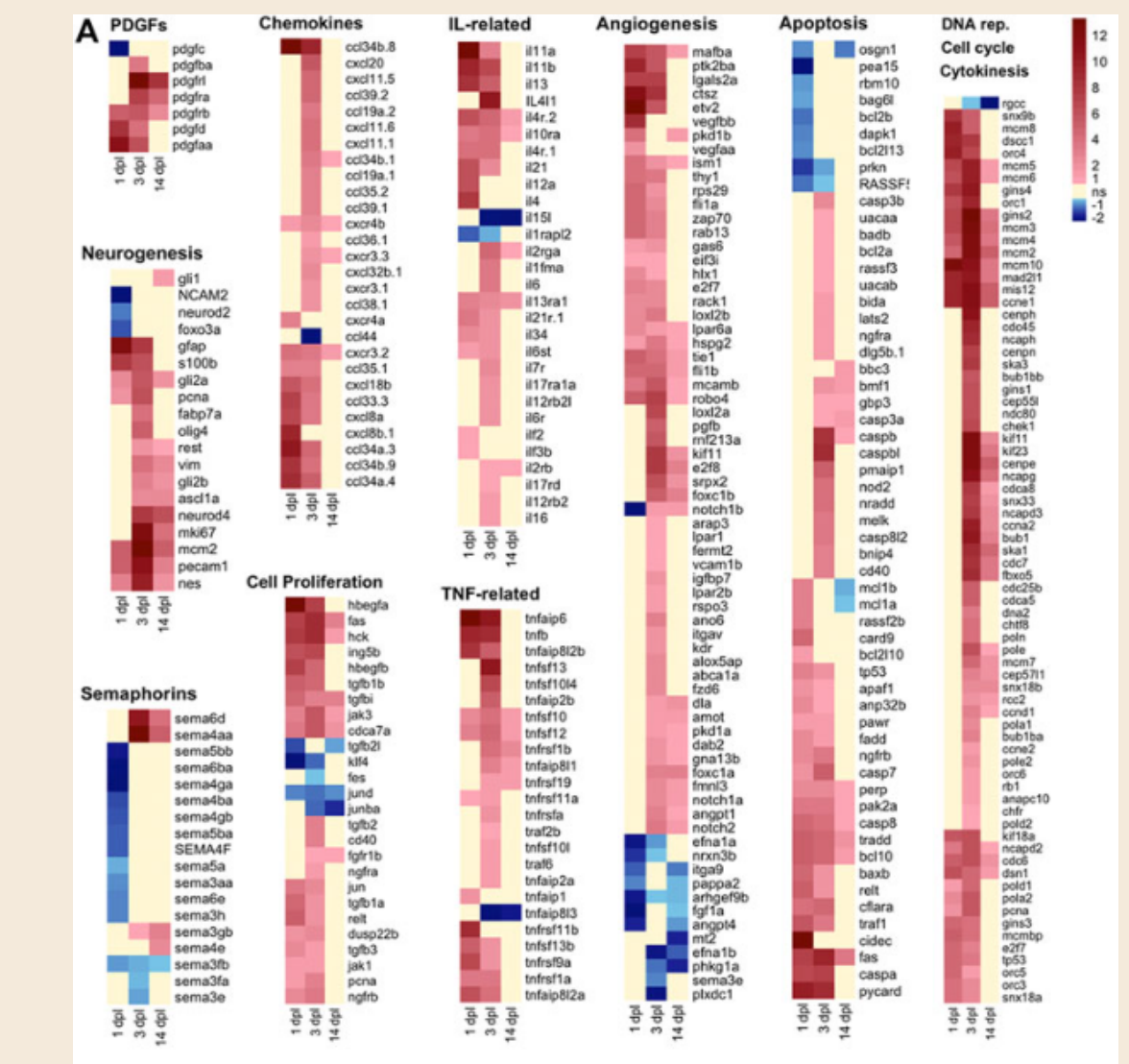
citation

Method

- Stab injury was performed in 6–10 month-old wild-type zebrafish. At 1, 3 and 14 dpl of stab injury, telencephalon was extracted followed by RNA isolation and cDNA preparation
 - RNA Sequencing was followed by Transcriptomic analysis :
 - FASTQC quality assessment
 - HISAT2 alignment to reference genome
 - read count using HTSeq2
 - Normalization, transformation, and DEA using DESeq2
 - Functional Annotation using DAVID
 - GO term enrichment analysis for all three regeneration stages

	A	B
1	Supplementary Table 3: GO-BP terms enriched at three different stages	
2	Category	Term
3	GOTERM_BP	GO:0006412~translation
4	GOTERM_BP	GO:0043604~amide biosynthetic process
5	GOTERM_BP	GO:0043043~peptide biosynthetic process
6	GOTERM_BP	GO:0006518~peptide metabolic process
7	GOTERM_BP	GO:0006364~rRNA processing
8	GOTERM_BP	GO:0022618~ribonucleoprotein complex assembly
9	GOTERM_BP	GO:0042273~ribosomal large subunit biogenesis
10	GOTERM_BP	GO:0042255~ribosome assembly

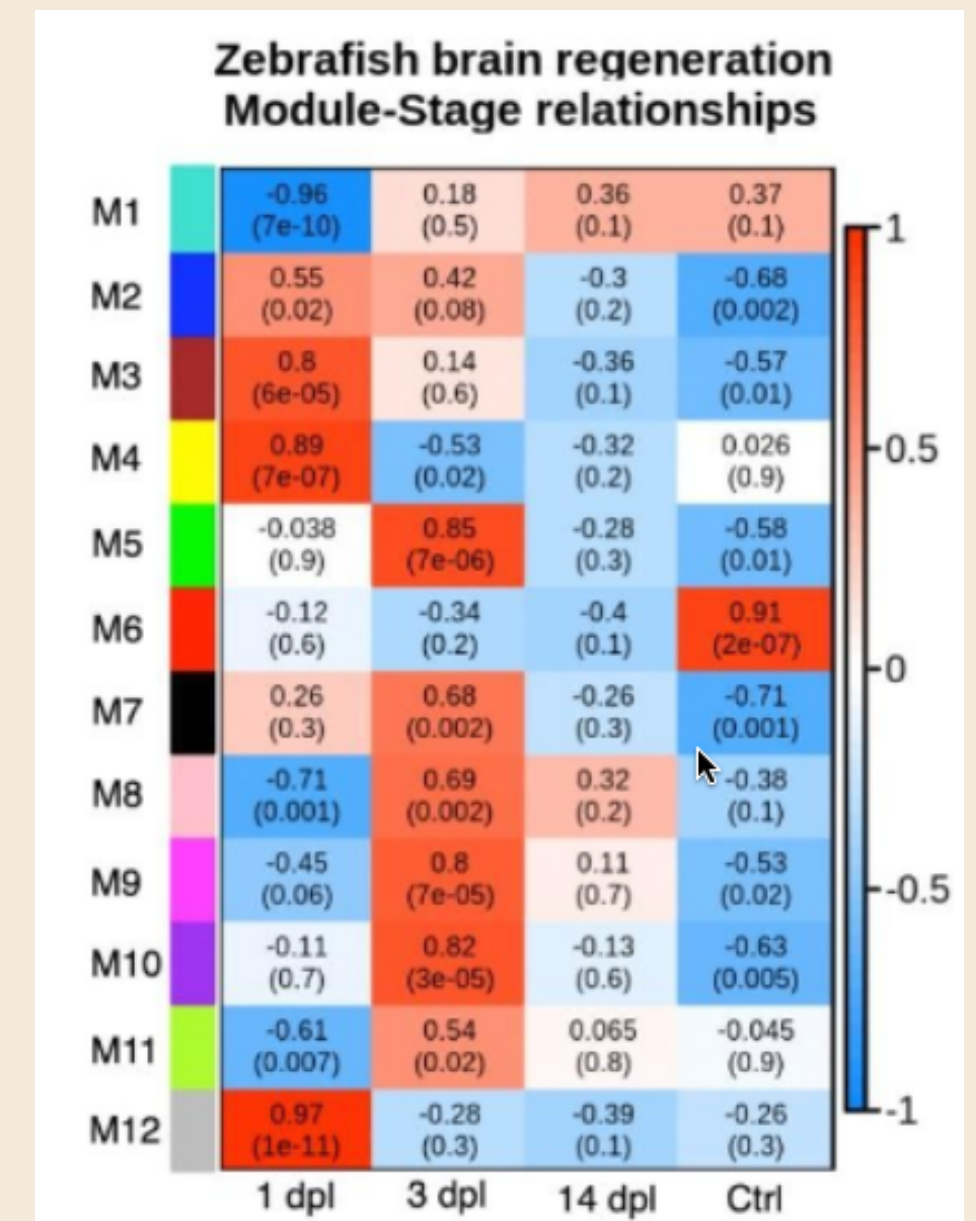
	A	B
1	Category	Term
2	GOTERM_BP	GO:0006260~DNA replication
3	GOTERM_BP	GO:1903047~mitotic cell cycle process
4	GOTERM_BP	GO:0030097~hemopoiesis
5	GOTERM_BP	GO:0050900~leukocyte migration
6	GOTERM_BP	GO:0048534~hematopoietic or lymphoid organ deve
7	GOTERM_BP	GO:0002520~immune system development
8	GOTERM_BP	GO:0000280~nuclear division
9	GOTERM_BP	GO:0035556~intracellular signal transduction
10	GOTERM_BP	GO:0006270~DNA replication initiation



Heatmaps of log2FoldChanges of selected genes across three stages of brain regeneration. Each column represents a time point and each row shows a single gene

Weighted Gene Co-expression Network Analysis (WGCNA)

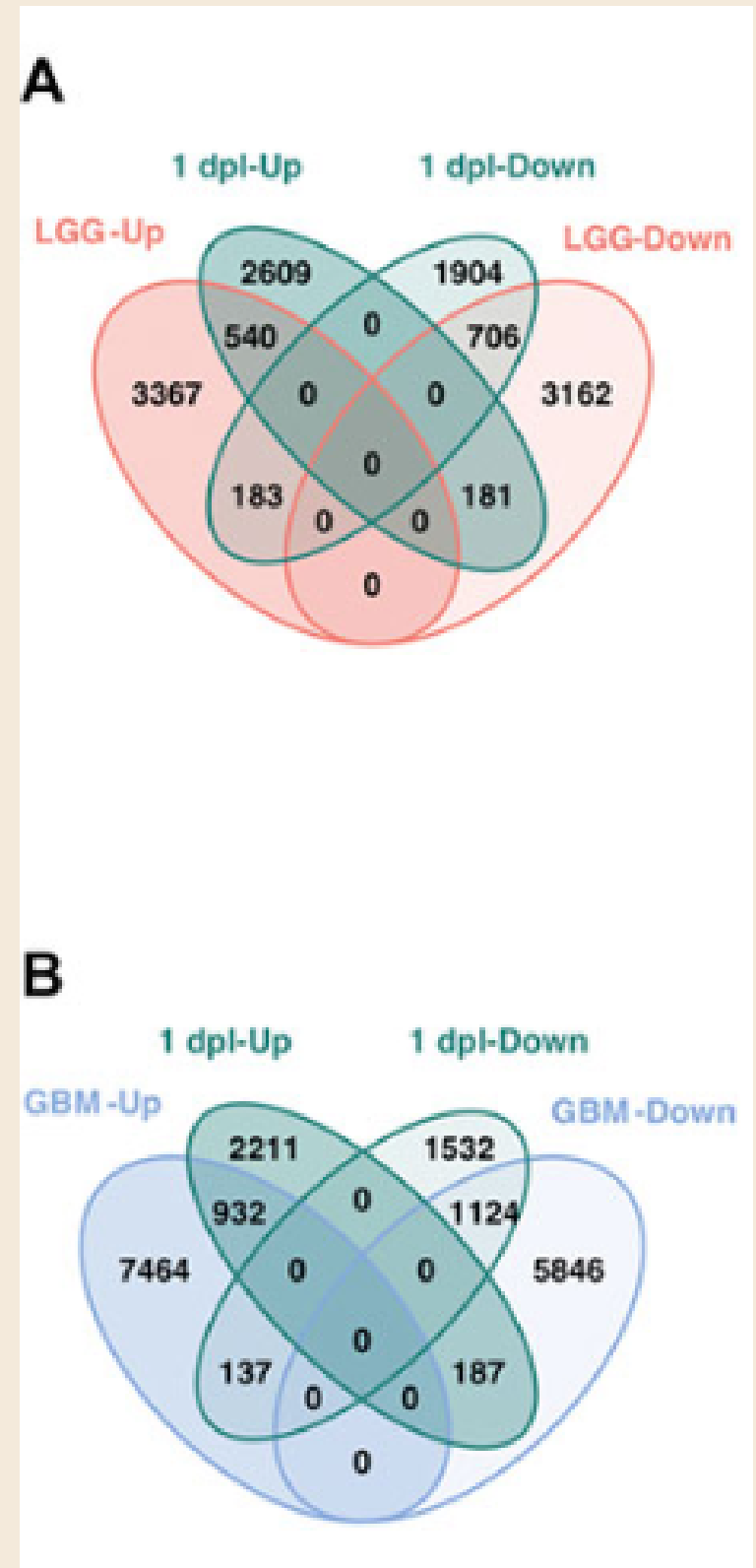
- Expression of the genes was clustered in nine modules (M1-M5 & M7-M10)
- Genes in these modules revealed expression patterns that distinguished one stage of regeneration from the other
- GO term enrichment analysis of the genes in these modules gave similar results to that of DEGs in each regenerative stage
- M1 and M3 showed expression patterns similar to 1dpl
- M5 and M10 similarly showed a pattern specific to 3 dpl
- There was no module specific to 14dpl, as it was similar to control
- These results show that events occurring during brain regeneration display stage specific patterns



The relationship between a module and a stage is the Pearson correlation coefficient between that module's eigengene score and the dummy binary variable representing the belonging of samples to that stage. The eigengene of a module is defined as the first principal component of the expression matrix projected on that module.

Early wound healing stage 1dpl vs cancer

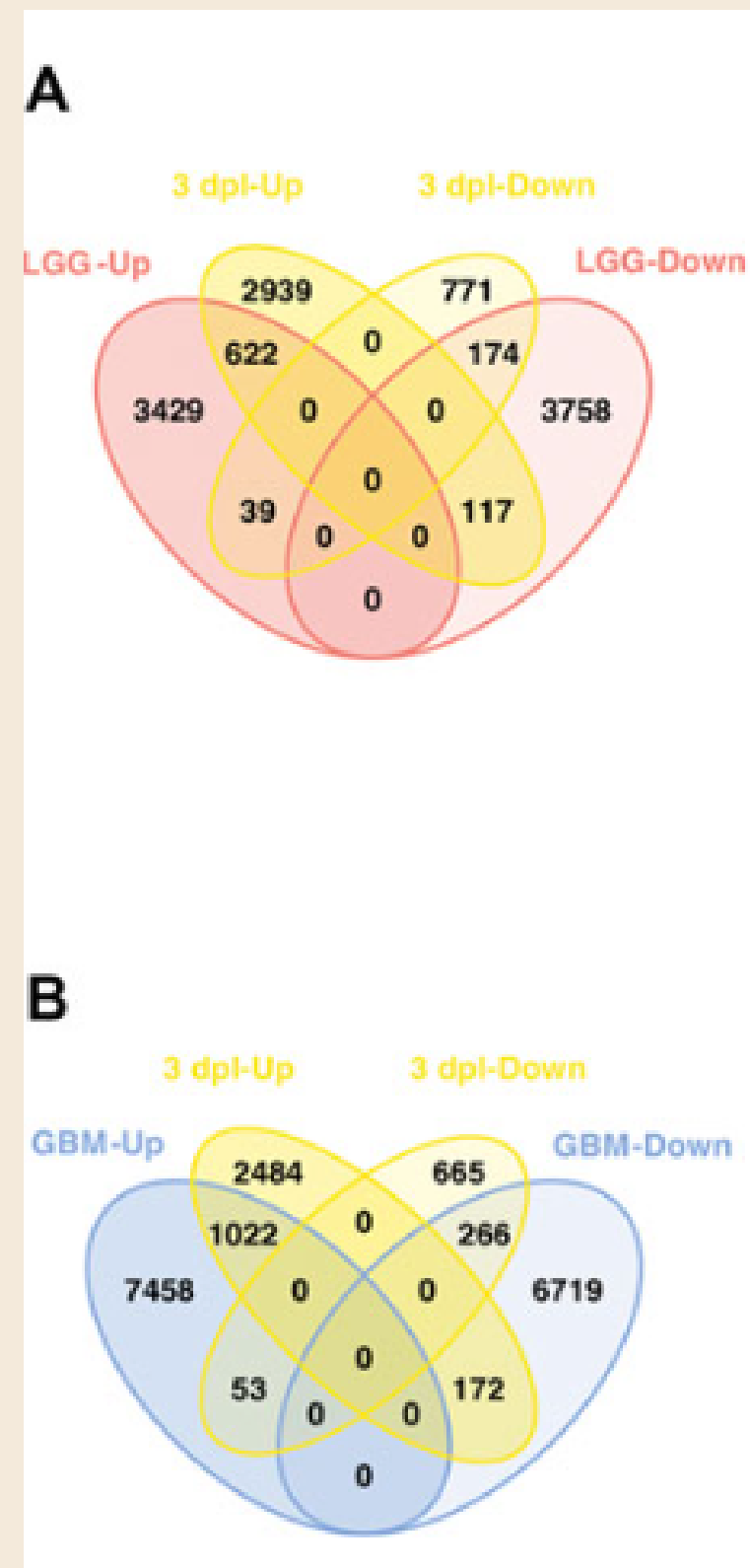
- DEGs at 1dpl were intersected with DEGs of LGG and GBM.
- 1,610 genes were shared with LGG.
- Between 1 dpl and GBM, the number of shared genes increased to 2,380. 2056 of which were regulated in the same direction and included majority of the genes shared between 1 dpl and LGG.
- Thus early wound healing stage of regeneration is more similar to GBM than to LGG at the transcriptional level.
- This was followed by functional annotation of shared genes using GO and KEGG, showing that early wound healing stage of brain regeneration is similar to brain cancer with respect to induction of metabolism and neurogenesis.



Proliferative stage

3dpl vs cancer

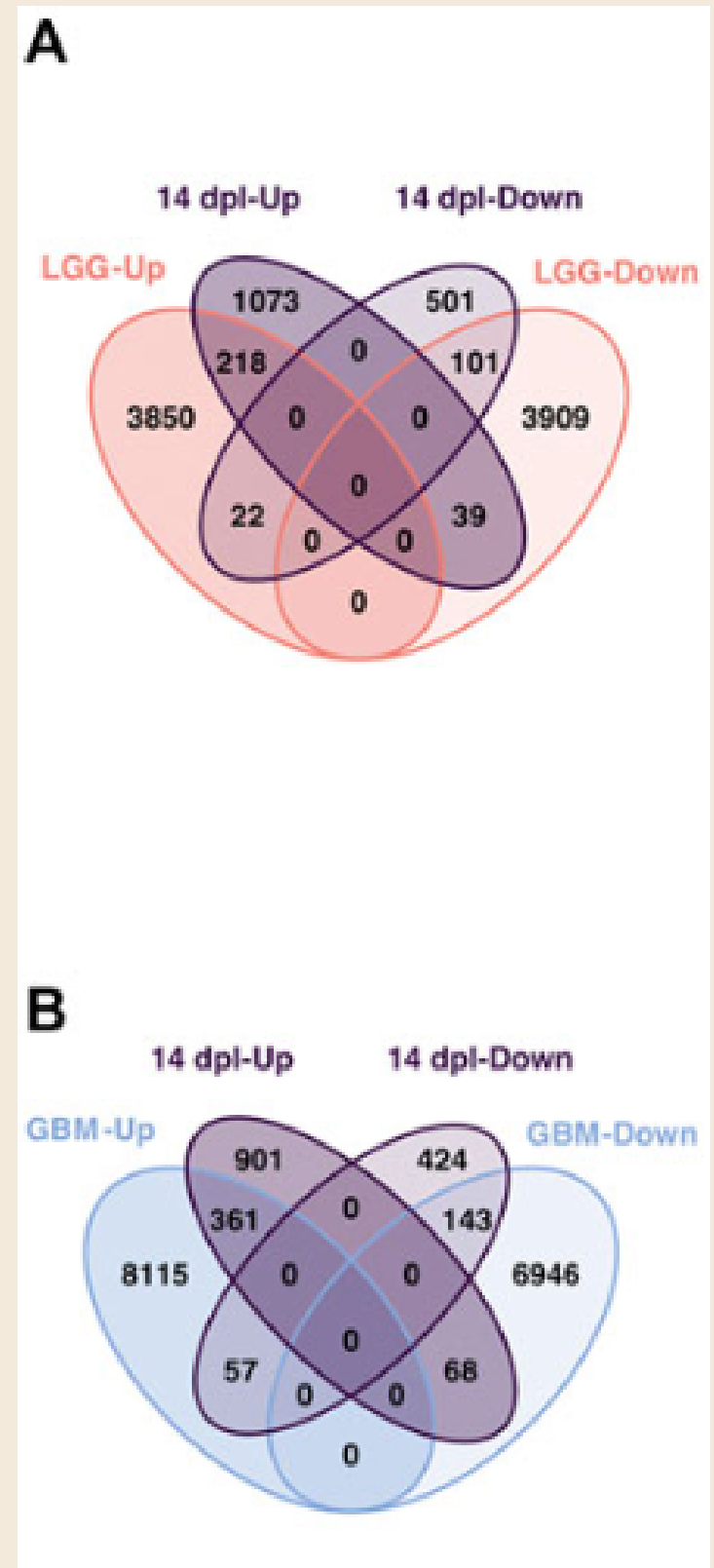
- DEGs at 3dpl were intersected with DEGs of LGG and GBM.
- 952 genes were shared with LGG. These genes involved the proliferation and glial markers mki67, pcna, several mcm genes and gfap, which were all Up-regulated.
- Between 1 dpl and GBM, the number of shared genes were 1513.
- GO terms were supported by KEGG pathway enrichment analysis, which showed that shared DEGs were enriched in various pathways related to cell proliferation and DNA repair.
- Thus, early Proliferative Stage of Brain Regeneration is Similar to LGG/GBM with Respect to Active Proliferation.



Differentiation stage

14dpl vs cancer

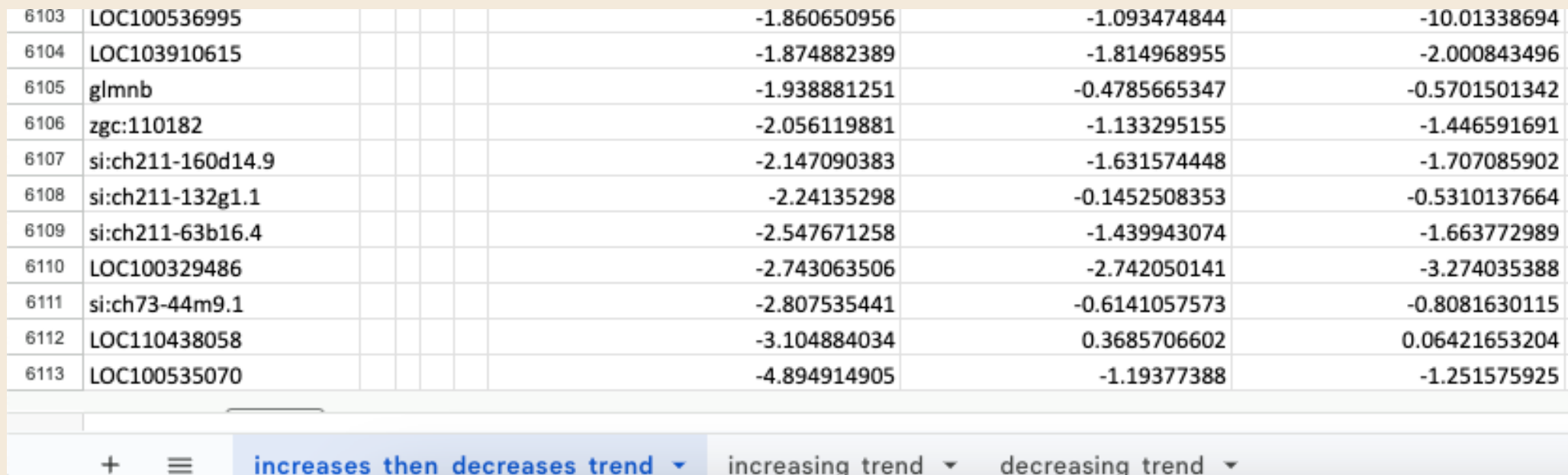
- DEGs at 14dpl were intersected with DEGs of LGG and GBM.
- 380 genes were shared with LGG.
- Between 1 dpl and GBM, the number of shared genes were 629.
- A number of GO-BP terms related to development and morphogenesis including nervous system development, neuron differentiation and angiogenesis were found. Several cancer-related pathways were enriched in DEGs between 14 dpl and LGG/GBM.
- Thus, developmental and morphogenetic processes are commonly activated during the differentiation stage of brain regeneration and brain cancer.



Interpreting and Comparing Our Results

- Immune Response is induced early after injury and starts to Decline after the Proliferative Stage
- Cell proliferation in cancer is similar to brain regeneration in early healing stages
- The number of shared and unique DEGs between cancer and regeneration was highest in 1dpl and 4dpl, and least in 7dpl
- Brain Regeneration Resembles Brain Cancer at its Earlier Stages and Diverges from Cancer, with regard to Opposite Regulation of Key Cancer-Related Genes

- Immune Response is induced early after injury and starts to Decline after the Proliferative Stage



The increase_decrease trend of our regeneration data has 6113 genes, almost double the amount of increasing_trend and decreasing_trend, with 3269 genes and 3182 genes respectively

- Cell proliferation in cancer is similar to brain regeneration in early healing stages

gene_name	log2FC_cancer	log2FC_day1	log2FC_day4	log2FC_day7
ftr43	2.597306793	2.722310304	2.263624094	1.96301926
ftr76	2.422748208	2.246296403	1.804271558	1.357825015
ftr33	1.668814437	1.824313525	0.3698155196	1.114422801
ftr85	0.9992403791	1.039253541	1.115992263	-0.000859598158

The finTRIM family of genes; ftr43, ftr76, ftr33, ftr85, have similar expression levels in cancer and early regeneration

- The number of shared and unique DEGs between cancer and regeneration was highest in 1dpl and 4dpl, and least in 7dpl

1dpl - 23,587

4dpl - 25,853

7dpl - 22,979

1	gene_name	log2FC_cancer	log2FC_day1	log2FC_day4	log2FC_day7
23584	cldnb	2.57312944	-2.502515328		
23585	cdkn1cb	-1.220583242	-2.778216234		
23586	dusp4	0.3065995803	-2.836638431		
23587	LOC103911540	1.199096378	-7.007576229		
25851	si:ch211-284a16.2	-7.008314241		-1.783641263	
25852	LOC103911912	-7.66997159		-3.736537246	
25853	LOC100148920	-8.135187834		-1.857099928	
22976	prb1	0	0.6639589905	-0.6829837874	-3.728737327
22977	krt91	-0.6892728244	-1.919971869	-3.122833931	-3.803088235
22978	LOC100535543	1.323484666	0.5540705184	1.39292432	-4.896730373
22979	LOC100536995	1.410833052	-1.860650956	-1.093474844	-10.01338694

- Brain Regeneration Diverges from Cancer, with regard to Opposite Regulation of Key Cancer-Related Genes

These genes show opposite expression profiles. They must, therefore, play a key role in preventing cells from undergoing carcinogenesis

lpar1	4	0.9895604359	0.5112252538	0.2338938339	0.1380290125
rasgrp4	1	0.9082721694	0.003317846366	0.4023219387	0.2335806677
apaf1	5	876.1581583	0.4491055658	0.5709202677	0.4390887461

KEGG pathway - "pathways in cancer"

nkd2b	4	1.690638334	0.3811470801	-0.03787128231	0.2269667964
sfrp1a	6	1.337682522	0.1851010413	0.0005804257128	0.3013760075
rspo3	2	1.944559456	-0.3220540227	0.5531551625	0.179873823

Wnt pathway-related genes

Literary References

A novel brain tumour model in zebrafish reveals the role of YAP activation in MAPK- and PI3K-induced malignant growth

Marie Mayrhofer,¹ Victor Gourain,¹ Markus Reischl,² Pierre Auffaticati,³ Armin Jenett,³ Jean-Stephane Joly,³ Matteo Benelli,⁴ Francesca Demichelis,⁴ Pietro Luigi Poliani,⁵ Dirk Sieger,⁶ and Marina Mione^{1,4,*}

► Author information ► Article notes ► Copyright and License information ► Disclaimer

ABSTRACT

Somatic mutations activating MAPK and PI3K signalling play a pivotal role in both tumours and brain developmental disorders. We developed a zebrafish model of brain tumours based on somatic expression of oncogenes that activate MAPK and PI3K signalling in neural progenitor cells and found that HRAS^{V12} was the most effective in inducing both heterotopia and invasive tumours. Tumours, but not heterotopias, require persistent activation of phospho (p)-ERK and express a gene signature similar to the mesenchymal glioblastoma subtype, with a strong YAP component. Application of an eight-gene signature to human brain tumours establishes that YAP activation distinguishes between mesenchymal grade glioma in a wide The Cancer Genome Atlas (TCGA) sample set including glioblastomas (GBMs). This suggests that the activation of YAP might be an important event in brain development, promoting malignant versus benign brain lesions. Indeed, co-expression of YAP (YAP^{S5A}) and HRAS^{V12} abolishes the development of heterotopias and leads to

Dis Model Mech

Dis Model Mech

Brain Regeneration Resembles Brain Cancer at Its Early Wound Healing Stage and Diverges From Cancer Later at Its Proliferation and Differentiation Stages

Yeliz Demirci^{1,2,3} Guillaume Heger⁴ Esra Katkak^{1,2} Irene Papathodorou⁵ Alvis Brazma⁵ Gunes Ozhan^{1,2*}

¹ Izmir Biomedicine and Genome Center (IBG), Dokuz Eylul University Health Campus, Inciralti-Balcova, Izmir, Turkey
² Izmir International Biomedicine and Genome Institute (IBG-Izmir), Dokuz Eylul University, Inciralti-Balcova, Izmir, Turkey
³ Wellcome Sanger Institute, Hinxton, United Kingdom
⁴ École Centrale de Nantes, Nantes, France
⁵ European Molecular Biology Laboratory-European Bioinformatics Institute (EMBL-EBI), Cambridge, United Kingdom

Gliomas are the most frequent type of brain cancers and characterized by continuous proliferation, inflammation, angiogenesis, invasion and dedifferentiation, which are also among the initiator and sustaining factors of brain regeneration during restoration of tissue integrity and function. Thus, brain regeneration and brain cancer should share more molecular mechanisms at early stages of regeneration where cell proliferation dominates. However, the mechanisms could diverge later when the regenerative response terminates, while cancer cells sustain proliferation. To test this hypothesis, we exploited the adult zebrafish that, in contrast to the mammals, can efficiently regenerate the brain in response to injury. By comparing transcriptome profiles of the regenerating zebrafish telencephalon at its three different stages, i.e., 1 day post-lesion (dpl)-early



Published: 14 March 2018

DNA methylation-based classification of central nervous system tumours

David Capper, David T. W. Jones, Martin Sill, Volker Hovestadt, Daniel Schrimpf, Dominik Sturm, Christian Koelsche, Felix Sahm, Lukas Chavez, David E. Reuss, Annekathrin Kratz, Annika K. Wefers, Kristin Huang, Kristian W. Pajtler, Leonille Schweizer, Damian Stichel, Adriana Olar, Nils W. Engel, Kerstin Lindenberg, Patrick N. Harter, Anne K. Braczyński, Karl H. Plate, Hildegard Dohmen, Boyan K. Garvalov, ... Stefan M. Pfister + Show authors

Nature 555, 469–474 (2018) | Cite this article

84k Accesses | 1422 Citations | 502 Altmetric | Metrics

Abstract

Accurate pathological diagnosis is crucial for optimal management of patients with cancer. For the approximately 100 known tumour types of the central nervous system, standardization of the diagnostic process has been shown to be particularly challenging—with substantial inter-observer variability in the histopathological diagnosis of many tumour types. Here we present a comprehensive approach for the DNA methylation-based classification of central nervous system tumours across all entities and age groups, and demonstrate its application in a routine diagnostic setting. We show that the availability of this method may have a substantial impact on diagnostic precision compared to standard methods, resulting in a change of diagnosis in up to 12% of prospective cases. For broader

Future Scope

- Identifying cellular signals that ensure timely ending of proliferation stage
- Compare DNA methylation profiles of the regenerating zebrafish
- Test the potential of specific molecular mechanisms of regeneration to stop cancer

